THE JOURNAL OF PHYSICAL CHEMISTRY A
A JOURNAL OF THE AMERICAN CHEMICAL SOCIETY

pubs.acs.org/JPCA Article

$S_2O_2^{q+}$ (q = 0, 1, and 2) Molecular Systems: Characterization and Atmospheric Planetary Implications

Published as part of The Journal of Physical Chemistry virtual special issue "Cheuk-Yiu Ng Festschrift".

Majdi Hochlaf,* Roberto Linguerri, Mohamed Cheraki, Tarek Ayari, Ridha Ben Said,* Raimund Feifel, and Gilberte Chambaud*

Cite This: *J. Phys. Chem. A* 2021, 125, 1958−1971 Read Online

ABSTRACT: We use accurate *ab initio* methodologies at the coupled cluster level ((R)CCSD(T)) and its explicitly correlated version ((R)CCSD(T)-F12) to investigate the electronic structure, relative stability, and spectroscopy of the stable isomers of the $[S_2O_2]$ system and of some of its cations and dications, with a special focus on the most relevant isomers that could be involved in terrestrial and planetary atmospheres. This work identifies several stable isomers (10 neutral, 8 cationic, and 5 dicationic), including *trigonal*-OSSO, *cis*-OSSO, and *cyc*-OSSO. For all these isomers, we calculated geometric parameters, fragmentation energies, and simple and double ionization energies of the neutral species. Several structures are identified for the first time, especially for the ionic species. Computations show that in addition to *cis*-OSSO and *trans*-OSSO proposed for the absorption in the near-UV spectrum of the Venusian atmosphere other S_2O_2, $S_2O_2^+$, and $S_2O_2^{2+}$ species may contribute. Moreover, the characterization of the stability of singly and doubly charged S_2O_2 entities can also be used for their identification by mass spectrometry and UV spectroscopy in the laboratory or in planetary atmospheres. In sum, the quest for the main UV absorber in Venus' atmosphere is not over, since the physical chemistry of sulfur oxides in Venus' atmosphere is far from being understood.

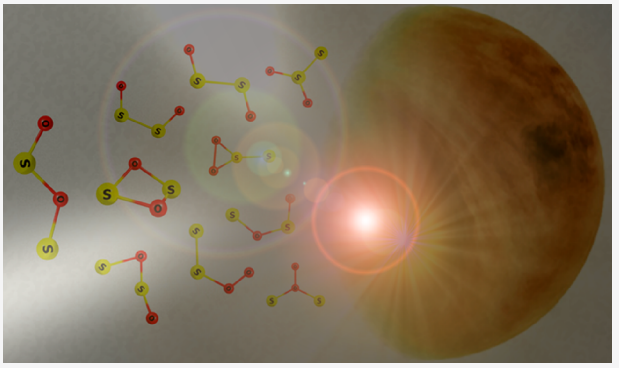

1. INTRODUCTION

Many sulfur compounds are present in the atmospheres of Earth and other planets like Venus[1] and moons like Io.[2] They play an important role in the gas phase chemistry of these media, where they are closely connected to the sulfur geochemical cycle. In Earth's atmosphere, they are of both natural and anthropogenic origins and contribute to the environmental pollution by forming acid rains and smog. Molecular species containing oxygen and sulfur are easily formed in volcanic and many other natural chemical processes. Within the Great Oxidation Event (GOE),[3] these oxygenated sulfur species were suggested to strongly influence Earth's earliest sulfur cycle, where they were involved in gas-phase reactions fixing the oxidation state of sulfur.[4] Also, in the atmospheres of Venus and Io, there are relatively high concentrations of sulfur oxides (SO and SO_2).[5] For instance, SO is the second most abundant sulfur oxide in the Venusian atmosphere just after SO_2: 7−30 ppb for SO and 30−500 ppb for SO_2 at an altitude of 64 km near the equator. In addition, the atmosphere of Io is composed of 90% sulfur dioxide.[6−8]

As sulfur monoxide (SO) is a key intermediate in the oxidation of sulfur in natural media, one can expect that the SO dimer (S_2O_2) could be present as well. In 2012, the lowest-energy S_2O_2 isomer (i.e., the trigonal C_{2v} form) was thought by Krasnopolsky[9] to be formed in Venus' atmosphere based on a theoretical study by Marsden and Smith.[10] Instead, Frandsen et al.[11] have proposed in 2016 that the near-UV absorption (i.e., 320−400 nm) in Venus' atmosphere[12] is due to two different S_2O_2 isomers, *cis*-OSSO and *trans*-OSSO, which are formed in significant quantities and eliminated mainly by photolysis in the near-UV region. More recently, Wu et al.[13] supported such a conclusion after identification of four S_2O_2 isomers by IR and UV/vis spectroscopies complemented by quantum chemical computations. Nevertheless, the recent work on this subject by Pérez-Hoyos et al.[14] revealed that although S_2O and S_2O_2 provide the best agreement with the UV band in MESSENGER/MASCS observations, no perfect match is found, and the new estimate of the S_2O_2 density in Venus by Krasnopolsky seems to be too low.[15] In the last two

Received: December 23, 2020
Revised: February 12, 2021
Published: February 26, 2021

https://dx.doi.org/10.1021/acs.jpca.0c11407
J. Phys. Chem. A 2021, 125, 1958−1971

years, the controversy is still ongoing, with contradictory statements on the origin of the Venusian near-UV absorber.[16,17] In sum, "there is still a long way to undoubtedly identify Venus' UV absorber..." as stated by Pérez-Hoyos et al.[14]

In the laboratory, the S_2O_2 molecule was first observed in 1974 by Lovas et al.,[18] formed by a microwave discharge in SO_2. In their experiments, a planar *cis*-OSSO chain of C_{2v} symmetry with two double S−O bonds and a central S−S bond with partial double bond character was identified by microwave spectroscopy. Subsequent theoretical and experimental studies[10,19−28] confirmed this structure and showed the existence of other isomers of S_2O_2. The SCF+MPn (self-consistent-field + Møller−Plesset) calculations of Marsden and Smith[10] predicted a planar trigonal form of C_{2v} symmetry, resembling that of the SO_3 molecule, being the most stable one (of singlet multiplicity) and therefore lower in energy than the *cis*-OSSO isomer observed by Lovas et al.[18] They also found a *trans* structure (*trans*-OSSO) and a cyclic form with energies very close to that of the corresponding *cis* form and several other isomers at higher energies. As for the triplet states, Marsden and Smith[10] could identify several *cis*- and *trans*-OSSO and SOSO isomers close in energy to the above-mentioned singlet ones. Recently, Goodarzi et al.[23,24] realized a detailed study at the B3LYP/6-311G++(3df, 3pd) level to search the stable singlet and triplet isomers of S_2O_2 and the transition states connecting them. They also determined the dissociation channels leading to $[S_2 + O_2]$. Their study confirmed the previous predictions of stable isomers by Marsden and Smith.[10] The energetic order of the three most stable isomers (i.e., *trigonal*-OSSO, followed by *cis*-OSSO and then *trans*-OSSO) was later confirmed by Born−Oppenheimer DFT molecular dynamics simulations (BO−DFT-MD).[26] In 2018, Wu et al.[13] experimentally identified four S_2O_2 isomers trapped into Ar or N_2 cold matrices (at 15 K), namely, *cis*-OSSO, *trans*-OSSO, *cyc*-OSSO, and *cis*-SOSO. The first three ones were obtained by condensing gaseous SO or by 266 nm laser photolysis of the $S_2\cdots O_2$ complex trapped in these cold matrices. The fourth isomer, *cis*-SOSO, is formed via UV-light-induced (365 nm) intramolecular isomerization of *cis*-OSSO or *trans*-OSSO. These characterizations were performed using IR and UV/vis spectroscopy and *ab initio* structural and vibrational computations.

The detection of SO in Io's exosphere was evidenced via the identification of strong and persistent ion cyclotron waves associated with the SO^+ ion.[2] Another (weaker) signal corresponding to SO_2^+ ions is also measured. Both ions may be related to the S_2O_2 singly or multiply charged ionic species. In the Venusian atmosphere, the main atmospheric molecules CO_2, N_2, SO_2, H_2SO_4, and H_2O are dissociated by lightning at high temperatures into atoms, ions, and plasma, whose recombination forms a multitude of complex and exotic molecular species, including sulfur oxides (S_xO and S_xO_y).[29] Although the implication of sulfur-oxide-containing ions was suggested, their involvement is not proven yet because of the lack of information on the corresponding ions. To date, some other sulfur oxide dications, such as SO^{2+}[30] and SO_2^{2+},[31] were already characterized as stable species in the laboratory. Concerning the S_2O_2 ions, however, very few theoretical or experimental studies are available. These are limited to brief mentions in the works dealing with $S_2O_2^+$ in the review papers of Steudel[32,33] and to the determination of the ionization energy of S_2O_2 after recording the photoionization efficiency (PIE) and the photoelectron−photoion coincidence spectrum (PEPICO) of this molecule by the Ng's group[34] and by Cheng and Hung.[35] The $S_2O_2^+$ ions were also observed in a mass spectrum experiment following electron impact of a microwave discharge of gaseous SO_2.[36]

In this work, we carry out a systematic study, using *ab initio* quantum chemistry methods, to determine the stable structures of the $S_2O_2^{q+}$ (q = 0, 1, and 2) molecular species and the pattern of their lowest excited electronic states. We also considered the formation (and decomposition) reactions of these species from the corresponding diatom/diatom and atom/triatom combinations. Moreover, we discussed the possible role of these species in sulfur oxide rich planetary atmospheres. In addition to singly charged ions, the presence of molecular doubly charged ions (e.g., N_2^{2+}, O_2^{2+}, and CO_2^{2+}) in the upper planetary atmospheres (e.g., upper Martian or Venusian atmospheres) was confirmed,[37,38] where their densities are strongly influenced by the solar radiation, the escape from ionosphere and the reactive ion−molecule processes they undergo therein. Our work should motivate revising the actual planetary atmospheric models to include $S_xO_y^{q+}$ (q = 0, 1, and 2) species.

2. COMPUTATIONAL DETAILS

All calculations were performed using the MOLPRO (version 2015) suite of *ab initio* programs.[39] First, we determined the stable forms of $S_2O_2^{q+}$ (q = 0, 1, and 2) and then the pattern of their electronic states. Indeed, the structures of the different isomers of neutral and charged S_2O_2 were obtained by performing a series of geometry optimizations for these species in their low-energy states, starting from a rather large set of different starting geometries. Many of these states and molecular geometries turned out to be first- or higher-order-saddle points and were discarded. Normal mode analysis for some of them also gave valuable hints on how these molecular structures had to be distorted in order to reach genuine minima on the PES. For the neutral species, previous works showed that the electronic ground states are of singlet spin multiplicity. Thus, we considered the lowest singlet potential energy surface (PES) of neutral $[S_2O_2]$. For the singly charged ions $[S_2O_2]^+$, we searched for minimal structures in the lowest doublet PES. For the $[S_2O_2]^{2+}$ dications, we performed such computations for both the lowest singlet and triplet PESs. The strategy consists in identifying the stable forms for the neutral system, then removing one and two electrons from these neutral isomers to find the respective stable cationic and dicationic species and the corresponding ionization energies. In all cases, the harmonic frequencies (all positive) were calculated to validate the minimal nature of the optimized forms.

For the ground states of the neutral and cationic species, the electronic calculations were conducted with the (partially spin restricted) coupled-cluster singles and doubles plus perturbative triples (R)CCSD(T) method[40−42] and its explicitly correlated version (R)CCSD(T)-F12.[43,44] Beforehand, the mono-configurational nature of $[S_2O_2]^{q+}$ (q = 0, 1, and 2) ground states was verified by calculations using the Complete Active Space Self-Consistent Field (CASSCF) method.[45,46] These calculations have shown that the wave functions of the electronic ground states of these isomers can be described by one dominant electronic configuration (CI coefficient > 90%). For these (R)CCSD(T) calculations, the choice of the aug-cc-pV(T+d)Z[47−49] basis set is a good compromise between

https://dx.doi.org/10.1021/acs.jpca.0c11407
J. Phys. Chem. A 2021, 125, 1958−1971

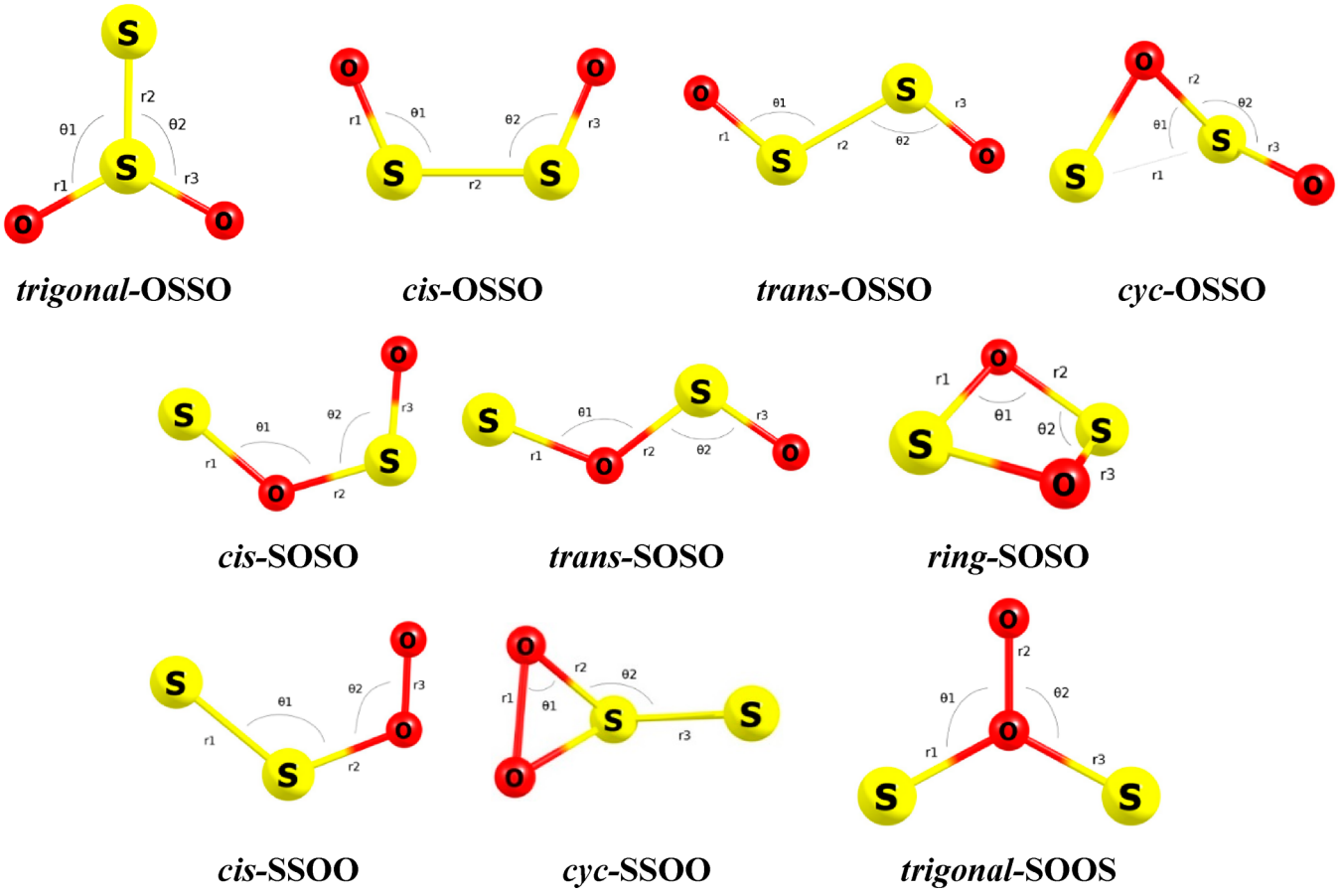

Figure 1. Possible stable isomeric forms of $S_2O_2^{q+}$ (q = 0, 1, and 2) with the definition of their geometric parameters given in Tables 1, 3, and 5.

computational time and accuracy. This atomic basis set includes the so-called "tight-d" functions which should be included in the standard set for a good description of sulfur-containing molecules. Subsequently, these structures were reoptimized with the (R)CCSD(T)-F12 method in conjunction with the cc-pVTZ-F12 basis set[50] and the appropriate MOLPRO default choices for the density fitting and resolution of identity basis sets.[51−53]

For the computations of the excited states, we used the CASSCF approach[45,46] followed by the MRCI (Multi-Reference-Configuration-Interaction) method,[54−56] where the atoms are described by the aug-cc-pV(Q+d)Z basis set. The oscillator strengths between relevant electronic states are calculated at the CASSCF level to complete the interpretation of the electronic spectra. At the CASSCF level, the electronic states are computed according to the state-average procedure, as implemented in MOLPRO. Here, the core and the three lowest valence orbitals are considered inactive, while the remaining valence orbitals form the active space. In the MRCI computations, all configurations with coefficients larger than 0.01 in the expansion of the CASSCF wave functions were used as reference states. This leads, for instance, to consider ~5.5 × 10^7 (~3 × 10^9) contracted (uncontracted) Configuration State Functions (CSFs) per C_s symmetry.

3. RESULTS AND DISCUSSION

As chalcogen elements, oxygen and sulfur each have six electrons in their valence shell. In contrast to most molecules with an even number of electrons which have a singlet electronic ground state, the O_2, S_2, and SO diatomics each have a triplet ground state (of $^3\Sigma_{(g)}^-$ space symmetry). Via interactions of identical dimers or interaction between S_2 and O_2, tetramers of these systems (O_4, S_4, or S_2O_2) can be formed. Such molecular systems exist in singlet or multiplet electronic states and their structures have been already the subject of several theoretical and experimental works. On the basis of *ab initio* calculations,[57−64] a cyclic structure was proposed for O_4, which was not confirmed experimentally. The covalently bonded cyclic O_4 (a cycle with four single O−O bonds) corresponds to an electronically excited species, while the ground state of O_4 is rather a van der Waals complex.[59,65] For S_4, several stable structures were predicted, with a great debate as to whether the "closed" D_{2h} cyclic or the "open" C_{2v} chain structure is the lowest energy one.[66] Compared to O_4 and S_4, there are additional difficulties to find the stable structures of S_2O_2 because of the larger number of possible isomers. The most stable S_2O_2 structures may result from the interaction of two SO units connected via sulfur atoms, or via oxygen, or via sulfur and oxygen or also via the interaction between S_2 and O_2. As a result, S_2O_2 tetramers can be found as cycles, *cis*-chains, or *trans*-chains or they can adopt branched structures of C_{2v}, C_s, or C_1 symmetry with a large variety of bonds. Figure 1 displays the probable stable structures of the S_2O_2 dimer. They can be gathered into different groups according to the type of bonding: for the OS−SO group of molecules characterized by a central S−S bond, 4 isomers are identified, namely, *cis*-OSSO (in C_{2v}), *trans*-OSSO (in C_{2h}), *cyc*-OSSO (in C_1), and *trigonal*-OSSO (in C_{2v}). For the SO−SO group of molecules, characterized by a central S−O bond,

https://dx.doi.org/10.1021/acs.jpca.0c11407
J. Phys. Chem. A 2021, 125, 1958−1971

Table 1. Geometric Parameters at Equilibrium Calculated at the (R)CCSD(T)/aug-cc-pV(T+d)Z and (R)CCSD(T)-F12/cc-pVTZ-F12 Level for the $[S_2O_2]$ Stable Isomers in Their Singlet Electronic Ground State and of Some Low-Lying Triplet States[a]

method	r_1	r_2	r_3	θ_1	θ_2	θ_3	E	E_R
				trigonal-OSSO(X^1A_1)				
this work[b]	2.716	3.558	2.716	120.3	120.3	0.0	−945.71660248	0.0
this work[c]	2.697	3.533	2.697	120.3	120.3	0.0	−945.81522461	0.0
calcd[d]	2.708	3.557	2.708		120.4			0.0
calcd[e]	2.695	3.527	2.695		120.5			0.0
calcd[f]	2.710	3.557	2.710		120.2			0.0
				trigonal-OSSO(1^3A_1)				
this work[c]	2.771	3.903	2.771	116.6	116.6	0.0	−945.69094438	3.38
				cis-OSSO(X^1A_1)				
this work[b]	2.795	3.828	2.795	113.1	113.1	0.0	−945.70214847	0.39
this work[c]	2.774	3.787	2.774	113.6	113.6	0.0	−945.79749051	0.48
calcd[d]	2.778	3.806	2.778	115.6	115.6	0.0		0.26
calcd[e]	2.781	3.650	2.781	114.3	114.3	0.0		0.58
calcd[f]	2.789	3.829	2.789	113.4	113.4	0.0		0.50
exp[g]	2.756	3.826	2.756	112.7	112.7	0.0		
exp[h]	2.772	3.800	2.772	113.0	113.0	0.0		
				cis-OSSO(1^3B_2)				
this work[c]	2.789	4.351	2.789	100.1	100.1	0.0	−945.75938827	1.52
				cis-OSSO(1^3A_1)				
this work[c]	3.032	3.880	3.032	99.6	99.6	0.0	−945.61913068	5.33
				trans-OSSO(X^1A_g)				
this work[b]	2.804	3.855	2.804	110.1	110.1	180.0	−945.69729706	0.52
this work[c]	2.784	3.814	2.784	110.2	110.2	180.0	−945.79231714	0.62
calcd[d]	2.790	3.831	2.790	110.7	110.7	180.0		0.38
calcd[e]	2.796	3.667	2.796	109.2	109.2	180.0		0.58
calcd[f]	2.799	3.863	2.799	110.1				0.59
				trans-OSSO(1^3B_u)				
this work[c]	2.803	4.191	2.803	103.9	103.9	180.0	−945.76175553	1.45
				trans-OSSO(1^3B_g)				
this work[c]	2.812	4.195	2.812	108.9	108.9	180.0	−945.72045234	2.58
				cyc-OSSO(X^1A)				
this work[b]	3.938	3.362	2.732	76.1	112.7	106.2	−945.68988577	0.73
this work[c]	3.949	3.364	2.714	76.2	115.6	100.8	−945.78497146	0.82
calcd[d]	3.098	3.347	2.721					0.74
calcd[e]	3.085	3.377	2.714					0.54
calcd[f]	3.992	3.364	2.725	76.4	115.9	101.1		0.77
				cis-SOSO(X^1A')				
this work[b]	3.131	3.057	2.756	123.3	110.9	0.0	−945.66831152	1.31
this work[c]	3.117	3.029	2.736	123.6	111.1	0.0	−945.76026261	1.49
calcd[d]	3.164	2.965	2.735	128.7	113.8			1.24
calcd[e]	3.630	2.750	2.682	136.8	117.0			1.41
calcd[f]	3.129	3.050	2.750	123.4	111.3			1.33
				cis-SOSO($1^3A'$)				
this work[c]	3.084	3.255	2.756	118.5	110.1	0.0	−945.74363064	1.95
				cis-SOSO($1^3A''$)				
this work[c]	3.138	3.129	2.765	119.8	109.2	0.0	−945.73374344	2.22
				trans-SOSO(X^1A')				
this work[b]	3.154	3.094	2.752	120.5	107.7	180.0	−945.65864816	1.58
this work[c]	3.139	3.067	2.733	120.7	107.9	180.0	−945.75045532	1.76
calcd[d]	3.189	2.968	2.735	127.4	110.1	180.0		1.48
calcd[e]	3.803	2.745	2.682	124.0	114.9	180.0		1.59
calcd[f]	3.147	3.087	2.748	120.6	108.1			1.58
				trans-SOSO($1^3A'$)				
this work[c]	3.096	3.225	2.752	109.6	105.7	180.0	−945.74764807	1.84
				trans-SOSO($1^3A''$)				
this work[c]	3.134	3.151	2.748	119.2	105.1	180.0	−945.73031510	2.31
				ring-SOSO(X^1A_1)				
this work[b]	3.228	3.228	3.229	89.0	84.4	26.9	−945.62018450	2.62
this work[c]	3.205	3.205	3.205	88.9	84.6	26.7	−945.71285484	2.78

https://dx.doi.org/10.1021/acs.jpca.0c11407
J. Phys. Chem. A 2021, 125, 1958−1971

Table 1. continued

method	r_1	r_2	r_3	θ_1	θ_2	θ_3	E	E_R
				ring-SOSO(X^1A_1)				
calcd[e]	3.245	3.245	3.245	95.8	83.4			1.77
				cyc-SSOO(X^1A)				
this work[b]	2.905	3.148	3.556	62.5	113.3	102.9	−945.61072743	2.88
this work[c]	2.890	3.122	3.533	62.4	113.3	103.0	−945.70390146	3.03
calcd[d]	2.735	2.966	3.164					
calcd[e]	2.682	2.750	3.631					
calcd[f]	2.762	3.008	3.163					
				cis-SSOO(X^1A')				
this work[b]	3.556	4.319	2.351	82.0	98.1	0.0	−945.60074514	3.15
this work[c]	3.530	4.222	2.340	83.3	99.1	0.0	−945.68971912	3.41
calcd[d]	3.547	3.185	2.446					3.09
				cis-SSOO($1^3A'$)				
this work[c]	3.545	4.755	2.312	82.6	97.5	0.0	−945.68766024	3.47
				trigonal-SOOS(X^1A_1)				
this work[b]	3.202	2.586	3.202	118.3	118.3	0.0	−945.46052055	6.97
this work[c]	3.186	2.568	3.186	123.3	118.3	0.0	−945.54522340	7.35
calcd[d]	3.219	2.516	3.219	123.0		0.0		6.70

[a]Bond lengths are given in Bohr; angles are given in degrees as illustrated in Figure 1. θ_3 is the dihedral angle; E is the total energy in Hartree (E_h). E_R, given in eV, are the relative energies with respect to the energy of the lowest singlet form (*trigonal*-OSSO) with the given method in this work and in the referenced data. [b](R)CCSD(T)/aug-cc-pV(T+d)Z. [c](R)CCSD(T)-F12/cc-pVTZ-F12. [d]B3LYP/6-311++G(3df,3pd). E_R refers to the most stable form in these calculations.[24] [e]SCF-UMP3.[10] [f]CCSD(T)/cc-pV(T+d)Z.[11] [g]r_0 structure as deduced by microwave spectroscopy.[18] [h]r_e^{emp} empirical structure as deduced by millimeter- and submillimeter-wave spectroscopy.[27]

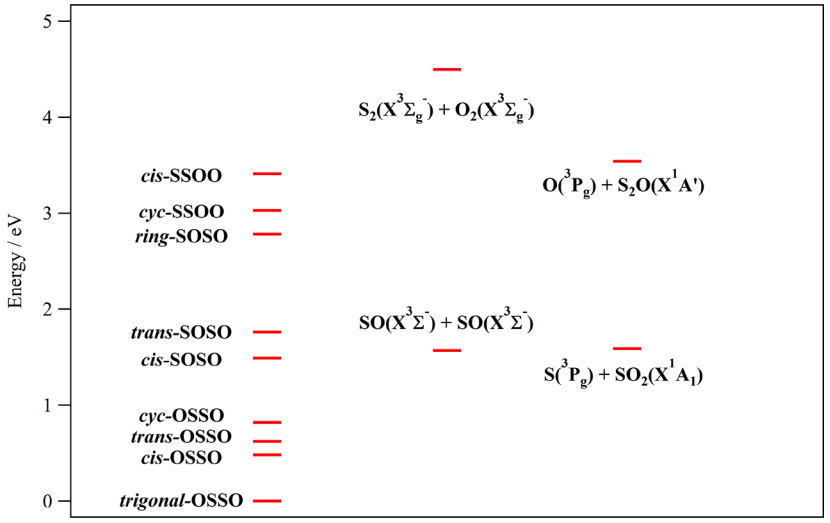

Figure 2. (R)CCSD(T)-F12/cc-pVTZ-F12 fragmentation energies (E_0 in eV, ZPE included) of the $[S_2O_2]$ stable structures into diatomic + diatomic and atomic + triatomic fragments. All molecular species are taken at their (R)CCSD(T)-F12/cc-pVTZ-F12 equilibrium geometries in their respective ground states. Cf. Table S1 for the characteristics of the fragments. *trigonal*-SOOS is not shown.

there are *cis*- and *trans*-isomers (in C_s) and a ring-shaped isomer in C_{2v} symmetry. For the SS−OO group of molecules, characterized by a central S−O bond separating S_2 and O_2 units, there are a *cis*-SSOO and a cyclic isomer, *cyc*-SSOO (in C_1). For the SO−OS group of molecules, characterized by a central O−O bond, there is a trigonal isomer, *trigonal*-SOOS (in C_{2v}).

3.1. The $[S_2O_2]$ Neutral System. *3.1.1. Energies and Spectroscopy of Stable Isomeric Structures of the $[S_2O_2]$ System.* The structural parameters at equilibrium geometry, as well as the absolute and relative energies of these stable isomers, are given in Table 1 and compared with existing data. We found 10 stable isomers on the ground singlet PES, which were already computed previously. No new isomers of singlet multiplicity are found. However, most of these isomers were not computed at high computational levels. For instance, the works of Goodarzi et al.[23,24] at the B3LYP level identified 9 forms for the $[S_2O_2]$ system which are approximately close to those given in Figure 1 and Table 1, except *ring*-SOSO. Frandsen et al.[11] presented only 6 forms obtained at the CCSD(T) level of theory. For the identified isomers, their results are very close to ours because of the similarities of the adopted approaches. Moreover, the high-energy isomers were only characterized at the B3LYP/6-311++G(3df,3pd). Thus, our work establishes the existence of 10 stable isomers. We also confirm the existence of 6 stable spin triplet ground states (below 5 eV over the reference singlet ground state) corresponding to 6 different isomers with geometries slightly different from those of the corresponding singlet. These triplets are located higher in energy, but in some cases (*trans*-

https://dx.doi.org/10.1021/acs.jpca.0c11407
J. Phys. Chem. A 2021, 125, 1958−1971

Table 2. Calculated Vertical Excitation Energies (ΔE in eV) and the Corresponding Wavelength (λ in nm) for Low-Lying Singlet Electronic States of Neutral $[S_2O_2]$ Isomer Systems as Computed at the MRCI/aug-cc-pV(Q+d)Z Level, Including the Davidson Correction[a]

isomer	*trigonal*-OSSO				*cis*-OSSO				*trans*-OSSO			
electronic state	X^1A_1	1^1A_2	1^1B_2	1^1B_1	X^1A_1	1^1A_2	1^1B_2	1^1B_1	X^1A_g	1^1A_u	1^1B_u	1^1B_g
ΔE	0.00	3.89[b]	5.17[b]	5.66[b]	0.00	2.77	3.92	4.48	0.00	2.49	3.43	4.09
f		0	0.00001	0.15906		0	0.10911	0.00516		0.00003	0.11461	0
λ		397	403	375		447	316	277		498	361	303
λ[c]		313	273	231		443	313	310		501	370	302
isomer	*cyc*-OSSO				*cis*-SOSO				*trans*-SOSO			
electronic state	X^1A	2^1A	3^1A	4^1A	X^1A'	$1^1A''$	$2^1A'$	$2^1A''$	X^1A'	$1^1A''$	$2^1A'$	$2^1A''$
ΔE	0.00	3.03	3.52		0.00	0.89	2.70	4.37	0.00	0.72	2.10	4.14
f		0.00067	0.00412			0.00001	0.18593	0.00484		0.00001	0.13081	0.00584
λ		409	352			1393	459	284		1722	590	299
λ[c]		397	305	263		971	375	287 338		1169	449	299 332
isomer	*cyc*-SSOO			*ring*-SOSO			*cis*-SSOO					
electronic state	X^1A	2^1A	3^1A	X^1A	2^1A	3^1A	X^1A'	$1^1A''$	$2^1A'$	$2^1A''$		
ΔE	0.00	0.73	0.98	0.00	1.68	2.66	0.00	2.45	2.77	2.85		
f		0.00010	0.00001		0.00090	0.00001		0.00022	0.00064	0		
λ		1698	1265		738	466		506	448	435		

[a]These energies are given with respect to the corresponding electronic ground state. The oscillator strength f is calculated between the lowest state of each isomer and the corresponding excited state. [b]Calculations at the CASSCF/aug-cc-pV(Q+d)Z level on CCSD(T)-F12/cc-pVTZ-F12 optimized geometry. [c]Calculations at the LR-CC2/aug-cc-pV(T+d)Z level on MRCI/cc-pV(T+d)Z optimized geometries.[11]

SOSO and *cis*-SSOO), they are very close to the corresponding singlets as previously established.[11,10,24]

Table 1 shows that the most stable structure is the C_{2v} *trigonal*-OSSO, as identified in previous theoretical works. In fact, to date this most stable form has not been observed in the laboratory. Instead, *cis*-OSSO isomer, the second most stable form, was already synthesized and characterized by microwave, millimeter- and submillimeter-wave spectroscopy, IR and UV spectroscopies.[18,27,13] Three other isomers (i.e., *trans*-OSSO, *cyc*-OSSO, and *cis*-SOSO) were recently formed by Wu et al.,[13] and their IR and UV/vis spectra were recorded.

We also identified 4 species of triplet spin multiplicity as electronic excited states. It is worth noting that the central bond in all triplet species is larger than in the corresponding singlet ground state. These triplets may play the role of intermediates during the reactive collisions between S/O + SO_2/S_2O, SO + SO, and S_2 + O_2. At least the Wigner−Witmer correlation rules reveal that only triplet $[S_2O_2]$ states correlate adiabatically to the ground state S/O + SO_2/S_2O asymptotes and that both $[S_2O_2]$ singlet and triplet potentials lead to the ground state SO + SO/S_2 + O_2. Their identification in the laboratory should help with the elucidation, after characterization, of their role in planetary atmospheres containing non-negligible amounts of sulfur oxides. For that purposes, our data for the triplet species and for the high energy isomers are accurate enough to assign the corresponding (ro-)vibrational spectra whenever measured.

3.1.2. Dissociation Energies of the Stable Isomers of the $[S_2O_2]$ System. The reaction energies of the molecular species of the $[S_2O_2]$ system have been evaluated for fragmentations into the most probable modes leading to diatom + diatom and atom + triatom (Figure 2, Tables S1 and S2). These energies were calculated by subtracting the energies of the tetramers from those of the associated fragments at equilibrium and corrected for the zero point vibrational energy (ZPE). These energies provide information on the relative stability of tetramer species compared to the corresponding dissociation limits. Indeed, the four low lying isomers (*trigonal*-OSSO, *cis*-OSSO, *trans*-OSSO, and *cyc*-OSSO) are located below the lowest dissociation asymptote (i.e., $S(^3P)$ + $SO_2(X^1A_1)$). Hence, they are stable against any kind of dissociation.

Table S2 shows that the reaction energies leading to two diatomic fragments are mostly around 0−1 eV, except those of *trigonal*-OSSO and *cyc*-SSOO, which are larger, and *cis*-SOSO, which has an almost zero fragmentation energy. Three isomers have negative dissociation energies. This shows a relative easiness in the breaking of the central S−O bond in this molecular system. This is also the case for *trans*-SOSO and *trigonal*-SOOS, which possess negative dissociation energies to form atomic and triatomic fragments on one side and diatomic fragments on the other (Table S2). In the case of close to zero or negative dissociation energies, the potential must have a barrier along the dissociation path. Such potential characteristics have been described for other C_{3v}/D_{3h} AX_3 tetratomic systems such as NO_3[+67] and CO_3.[68]

For the dissociation energies leading to atomic and triatomic fragments, the dissociation energies are in the 3−5 eV range, except the lowest isomer, *trigonal*-OSSO, with 1.59 eV. By comparing these results, we conclude that the external bonds of these tetramer molecules are generally stronger than the central ones, especially when the S=O bond has to be broken. For example, it is necessary to provide 5.13 eV to release an oxygen atom, but it takes only 0.04 eV to break the central bond and only 0.11 eV to release a terminal sulfur atom for the *cis*-SOSO isomer.

The dissociation energies of the triplet states are given in Table S2. Since the triplets are above the corresponding singlets, these energies are smaller, but in many cases they are positive confirming the stability of these states. Data in Figure 2 and Table S2 can help to discuss possible paths for the $2SO(X^3\Sigma^-) \rightarrow S(^3P) + OSO(X^1A')$ reaction, which should occur in the triplet potential energy surface at large interatomic separations. This reaction is endothermic (calculated here 0.07 eV (6.7 kJ/mol)), and we can deduce from Table S2 that a

https://dx.doi.org/10.1021/acs.jpca.0c11407
J. Phys. Chem. A 2021, 125, 1958−1971

Table 3. Total Energies and Optimized Geometric Parameters at the RCCSD(T)/aug-cc-pV(T+d)Z and RCCSD(T)-F12/cc-pVTZ-F12 Levels for Cationic $[S_2O_2]^+$ Isomers in Doublet Spin Multiplicity[a]

method	r_1	r_2	r_3	θ_1	θ_2	θ_3	E	E_R	AIE
				cis-OSSO$^+$(X^2B_1)					
RCCSD(T)	2.758	4.177	2.758	101.3	101.3	0.0	−945.33786749	0.00	9.91
RCCSD(T)-F12	2.739	4.127	2.739	101.8	101.8	0.0	−945.42891365	0.00	10.03
exp[b]									9.93 ± 0.02[c]
				trans-OSSO$^+$(X^2A_u)					
RCCSD(T)	2.764	4.103	2.764	106.3	106.3	180.0	−945.33472044	0.09	9.87
RCCSD(T)-F12	2.745	4.057	2.745	106.3	106.3	180.0	−945.42591997	0.08	9.97
				cis-SOSO$^+$(X^2A')					
RCCSD(T)	3.291	2.924	2.687	124.9	115.5	0.0	−945.33008434	0.21	9.20
RCCSD(T)-F12	3.244	2.870	2.681	126.2	115.2	0.0	−945.42002942	0.24	9.25
				trans-SOSO$^+$(X^2A'')					
RCCSD(T)	3.298	2.947	2.682	114.1	110.3	180.0	−945.32682451	0.30	9.03
RCCSD(T)-F12	3.278	2.928	2.664	114.1	110.4	180.0	−945.41656434	0.33	9.08
				trigonal-OSSO$^+$(X^2B_2)					
RCCSD(T)	2.677	3.731	2.677	114.8	114.8	0.0	−945.32457488	0.36	10.66
RCCSD(T)-F12	2.659	3.696	2.659	114.9	114.9	0.0	−945.41916705	0.26	10.77
				lin-OSSO$^+$ ($X^2\Pi_u$)					
RCCSD(T)	2.734	4.491	2.734	180.0	180.0		−945.29290014	1.22	11.13[d]
RCCSD(T)-F12	2.715	4.435	2.715	180.0	180.0		−945.38178404	1.28	11.31
				cyc-SSOO$^+$(X^2A')					
RCCSD(T)	2.965	3.052	3.748	60.9	109.5	101.4	−945.23237389	2.87	12.45
RCCSD(T)-F12	2.953	3.028	3.713	60.8	110.1	101.7	−945.32150753	2.92	12.61
				trigonal-SOOS$^+$(X^2B_2)					
RCCSD(T)	3.244	2.450	3.244	125.5	125.5	0.0	−945.10964609	6.21	9.55
RCCSD(T)-F12	3.226	2.433	3.226	125.7	125.7	0.0	−945.19199353	6.44	9.61

[a]E are given in Hartree. Bond lengths are given in Bohr, and angles are given in degrees. Relative energies (E_R in eV) with respect to the most stable cationic species and adiabatic ionization energies (eV) relative to their parent neutral singlet isomer are also given. [b]Photoionization efficiency spectroscopy.[35] [c]May also correspond to *trans*-OSSO AIE. See text. [d]Ionization from the *cis*-OSSO ground state.

path through the intermediate triplet *trans*-SOSO isomer is possible. Since this isomer is located at only 0.31 eV (30 kJ/mol) above the entrance channel, and since the geometry of the reactants, the products, and the *trans*-SOSO($1^3A'$) intermediate are very close, we conclude that this and the reverse reactions can proceed on the triplet potential energy surface via a small activation barrier with a rate constant in agreement with that obtained in the experiments of Murakami et al.[25] The singlet *trans*-SOSO(X^1A'), located 0.06 eV below the corresponding triplet, can also play a role in this reaction via spin−orbit interaction.

3.1.3. Excited Electronic States of $[S_2O_2]$. As mentioned in the Introduction, the identification of S_2O_2 species in the Venusian atmosphere is carried out after comparing the recorded near-UV absorption between 320 and 400 nm, which corresponds to an energy range of 3.10−3.87 eV. Since only some $[S_2O_2]$ forms were considered in the work of Frandsen et al.[11,17] and of Wu et al.,[13] we extended the computations of the pattern of the electronic states to all stable forms discussed above. Therefore, we calculated the vertical excitation energies and the corresponding wavelength (λ in nm) for all 10 singlet isomers of the neutral $[S_2O_2]$ system at the MRCI/aug-cc-pV(Q+d)Z level, including the Davidson correction. The data are given in Table 2.

According to Frandsen et al.[11,17] and of Wu et al.,[13] near-UV absorption transitions in the Venusian atmosphere are due to a mixture of *cis*- and *trans*-OSSO. From our investigations including excitation energies and oscillator strengths, reported in Table 2, *cis*-OSSO (transition $X^1A_1 - 1^1B_2$ at 316 nm), *trans*-OSSO (transition $X^1A_g - 1^1B_u$ at 361 nm), *trigonal*-OSSO (transition $X^1A_1 - 1^1B_2$ at 403 nm), and *cyc*-OSSO (transition $X^1A - 3^1A$ at 352 nm) are good candidates. Thus, we propose additional involvement of *cyc*-OSSO (symmetry C_1) and *trigonal*-OSSO (symmetry C_{2v}) for the assignment of the near-UV Venusian absorption band. Figure 2 shows that the formation of these high-energy isomers is favorable after reactive collisions between O_2 and S_2 and between O + S_2O. The vertical chemical composition of Venus reveals the presence of S_2, O_2, and S_2O species in addition to SO.[69,70]

3.2. Structure and Energetics of the Stable Isomers of the $[S_2O_2]^+$ Cation. *3.2.1. Stable Forms of the Cationic $[S_2O_2]^+$ System.* Starting from the 16 stable neutral structures (of singlet and triplet spin symmetries) we detached one electron and obtained 8 stable cationic species located in the lowest doublet potential energy surface. Their geometric characteristics are given in Table 3. They are named *cis*-OSSO$^+$, *trans*-OSSO$^+$, *cis*-SOSO$^+$, *trans*-SOSO$^+$, *trigonal*-OSSO$^+$, *lin*-OSSO$^+$, *cyc*-SSOO$^+$, and *trigonal*-SOOS$^+$ (i.e., five isomers belonging to the OSSO group (2 of C_{2v} symmetry, 1 of C_{2h} symmetry, 1 of $D_{\infty h}$, and 1 of C_1 symmetry) with a S−S bond, 2 isomers in the SOSO group (both of C_s symmetry) with a central S−O bond, and 1 isomer in the SOOS group (of C_{2v} symmetry), which has an O−O bond as found for the neutral form). The five lowest isomers are located very close in energy (E_R < 0.5 eV). This makes it difficult to determine the most stable form.

Although slight differences are observed between RCCSD(T)/aug-cc-pV(T+d)Z and RCCSD(T)-F12/cc-pVTZ-F12 relative energies, both methods agree that the most stable isomer is *cis*-OSSO$^+$, in which the central S−S bond is longer

https://dx.doi.org/10.1021/acs.jpca.0c11407
J. Phys. Chem. A 2021, 125, 1958−1971

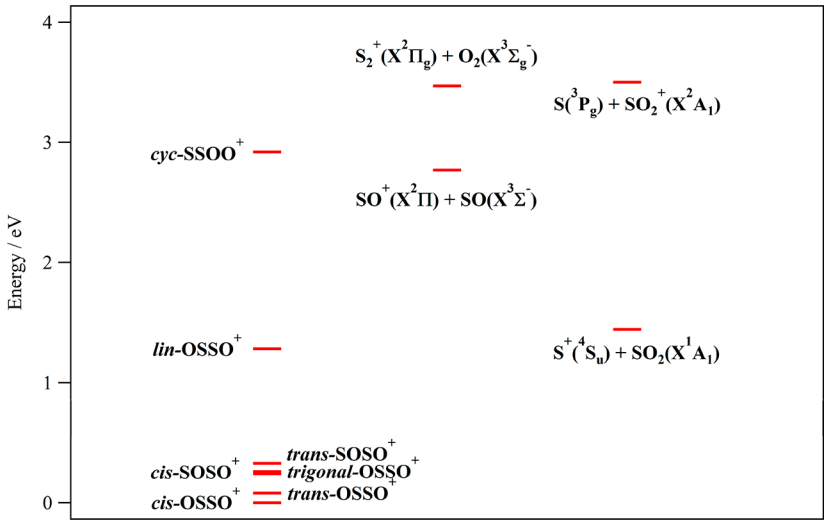

Figure 3. (R)CCSD(T)-F12/cc-pVTZ-F12 fragmentation energies (E_0 in eV, ZPE included) of the $[S_2O_2]^+$ stable structures into diatomic + diatomic and atomic + triatomic fragments. All molecular species are taken at their (R)CCSD(T)-F12/cc-pVTZ-F12 equilibrium geometries in their respective ground states. See Tables S1 and S3 for more details. *trigonal*-$SOOS^+(X^2B_2)$ is not shown. The ejection of O/O^+ from *cis*-$OSSO^+$ occurs for energies >5.7 eV (Table S3).

for the cation than for the neutral by 0.3 Bohr, which implies a loss of binding character of this bond. Indeed, Figure S1 shows that the highest occupied molecular orbital (HOMO) of *cis*-OSSO corresponds to a π orbital located between the two sulfur atoms. The removal of an electron from this MO is accompanied by a weakening of the S−S bond and its subsequent lengthening. The next stable one is the *trans*-$OSSO^+$ in which the S−S central bond is also increased by 0.3 Bohr compared to the neutral. Similar to *cis*-OSSO, the lengthening of the S−S bond is due to the ejection of an electron from a π-bonding MO, which is located between the two sulfur atoms. Starting from the *cis* bent isomer a stable *linear*-$OSSO^+$ form is found with an even longer central S−S bond of 4.43 Bohr. This state has a $^2\Pi_u$ space symmetry. In fact, the three isomers are located in the same lowest doublet $OSSO^+$ potential. Indeed, the $^2\Pi_u$ electronic state is doubly degenerate for linear geometries and the degeneracy disappears in the bent structures. The antisymmetric component of this $^2\Pi_u$ state correlates to the *cis*-$OSSO^+(^2B_1)$ and *trans*-$OSSO^+(^2A_u)$ forms. Moreover, the symmetric ones, corresponding to the first excited bent states, are coupled at linearity by Renner−Teller and spin−orbit couplings. Therefore, the spectroscopy of this weakly bound charge transfer tetratomic is extremely complex as discussed for $OMgOO^+$.[71]

Higher in energy, we found *cis*-$SOSO^+$ and *trans*-$SOSO^+$ in which the central O−S bond is shortened by 0.13 Bohr compared to the neutral form since it is antibonding in nature (Figure S1). For *trigonal*-OSSO, the detachment of one electron results in a change of the S−S−O angle from 119 to 115° and an increase of the S−S bond since the ionization occurs from a lone pair of the external sulfur (Figure S1). Similarly, the detachment of one electron from this lone pair does not significantly affect the structure of ionized *cyc*-OSSO. For *trigonal*-SOOS, there is a shortening of the O−O bond by 0.3 Bohr since the HOMO of the neutral isomer is antibonding. The two latter structures are lying at relative energies of >1 eV with respect to the most stable form.

3.2.2. Dissociation Energies of $[S_2O_2]^+$ Isomers. Figure 3 presents an energetic diagram of the stable forms for cationic S_2O_2 stable species, where we added the fragmentation energies producing $SO^+ + SO$, $S_2^+ + O_2$, and $S^+/+ SO_2/SO_2^+$ (all compounds being in their electronic ground state). The O_2^+ and O^+ production channels are located higher in energies (cf. Table S3). This figure shows that *cis*-, *trans*-, *lin*-, and *trigonal*-$OSSO^+$ and *cis*- and *trans*-$SOSO^+$ are located in energy below the lowest asymptote (i.e., $S^+(^4S_u) + SO_2(X^1A_1)$). They are stable with respect to fragmentations. As discussed above for neutrals, the reaction paths may have a potential barrier before reaching the asymptotic region especially for *cis*-, *trans*-, and *lin*-$OSSO^+$ upon ejection of S^+. This figure allows also discussing the formation of *cis*-, *trans*-, and *lin*-$OSSO^+$ after reactive collisions between $SO^+ + SO$ and that of *cyc*-$SSOO^+$ from $S_2^+ + O_2$. Indeed, the dissociation energies for the former ones are 2.77, 2.69, and 1.49 eV, respectively. These energies are typical for relatively strong charge transfer tetratomic complexes. The *cyc*-$SSOO^+$ system can be viewed as a barrierless product issued from the $S_2^+ + O_2$ reaction. We compute a moderate dissociation energy for *cyc*-$SSOO^+$ of 0.55 eV. Again, this is typical of charge transfer dissociation energies involving the OO moiety.[67,71,72] Therefore, in a planetary atmosphere where these neutral atoms, diatoms, triatoms, and their corresponding singly charged ions are present, one cannot exclude the formation and the existence of the less stable tetratomic ions in these media. As discussed above, microwave discharges in a gas mixture of argon and SO_2 or the condensation of gaseous SO or 266 nm laser photolysis of the $S_2\cdots O_2$ mixture followed by cold matrices trapping[13,17] do not necessary lead exclusively to the most stable *trigonal*-OSSO form but also to the less stable OSSO and SSOO chain forms. Obviously, one needs to consider all the cationic forms presently found for modeling such planetary atmospheres.

3.2.3. Adiabatic Ionization Energies of the $[S_2O_2]$ Species. Table 3 lists the adiabatic ionization energies (AIE) of the parent neutral singlet isomers. They are computed as the energy difference between that of the singly charged ion and that of the corresponding neutral system after considering the ZPE correction. Only the AIE of *cis*-OSSO was measured by Cheng and Hung[35] by means of a discharge flow and a photoionization mass spectrometer coupled to a synchrotron

https://dx.doi.org/10.1021/acs.jpca.0c11407
J. Phys. Chem. A 2021, 125, 1958−1971

Table 4. CASSCF/aug-cc-pV(Q+d)Z Vertical Excitation Energies (ΔE, in eV), Oscillator Strengths f, Dominant Electronic Configurations, and the CI Coefficient of the Corresponding Electronic Configuration (in Parentheses) for Isomers of the $[S_2O_2]^+$ Cationic System[a]

electronic state	ΔE	electronic configuration	f	electronic state	ΔE	electronic configuration	f
		cis-OSSO$^+$(X^2B_1)				*trans*-OSSO$^+$(X^2A_u)	
X^2B_1	0.00	(0.90) $(9b_2)^2(10a_1)^2(3b_1)^1(3a_2)^0$		X^2A_u	0.00	(0.91) $(2b_g)^2(9b_u)^2(10a_g)^2(3a_u)^1(3b_g)^0$	
1^2A_1	0.47 0.23[c]	(0.85) $(9b_2)^2(10a_1)^1(3b_1)^2(3a_2)^0$	0.00003	1^2A_g	0.37 0.28[c]	(0.86) $(2b_g)^2(9b_u)^2(10a_g)^1(3a_u)^2(3b_g)^0$	0.00003
1^4B_2	1.15	(0.93) $(9b_2)^2(10a_1)^1(3b_1)^1(3a_2)^1$		1^4B_u	1.05	(0.93) $(2b_g)^2(9b_u)^2(10a_g)^1(3a_u)^1(3b_g)^1$	
1^2B_2	1.66 1.55[c]	(0.74) $(9b_2)^2(10a_1)^1(3b_1)^1(3a_2)^1$	0	1^2B_u	1.57 1.65[c]	(0.74) $(2b_g)^2(9b_u)^2(10a_g)^1(3a_u)^1(3b_g)^1$	0
1^2A_2	1.74 2.05[c]	(0.86) $(9b_2)^2(10a_1)^2(3b_1)^0(3a_2)^1$	0.02543	1^2B_g	1.76 2.01[c]	(0.87) $(2b_g)^2(9b_u)^2(10a_g)^2(3a_u)^0(3b_g)^1$	0.03198
2^2B_2	2.77 2.68[c]	(0.78) $(9b_2)^1(10a_1)^2(3b_1)^2(3a_2)^0$	0	2^2B_u	3.01 2.83[c]	(0.73) $(2b_g)^2(9b_u)^1(10a_g)^2(3a_u)^2(3b_g)^0$	0
2^2A_2	3.22 2.75[c]	(0.87) $(9b_2)^2(10a_1)^0(3b_1)^2(3a_2)^1$	0.00135	2^2B_g	3.05 2.75[c]	(0.87) $(2b_g)^2(9b_u)^2(10a_g)^0(3a_u)^2(3b_g)^1$	0.00120
1^4A_1	3.83	(0.84) $(9b_2)^1(10a_1)^2(3b_1)^1(3a_2)^1$		1^4A_g	4.19	(0.82) $(2b_g)^2(9b_u)^1(10a_g)^2(3a_u)^1(3b_g)^1$	
		cis-SOSO$^+$(X^2A')				*trans*-SOSO$^+$(X^2A'')	
X^2A'	0.00	(0.93) $(5a'')^2(19a')^1(6a'')^0(20a')^0$		X^2A''	0.00	(0.91) $(19a')^2(5a'')^1(6a'')^0(20a')^0$	
$1^2A''$	0.05	(0.92) $(5a'')^1(19a')^2(6a'')^0(20a')^0$	0	$1^2A'$	0.21 0.20[c]	(0.93) $(19a')^1(5a'')^2(6a'')^0(20a')^0$	0
$1^4A'$	2.25	(0.92) $(5a'')^1(19a')^1(6a'')^1(20a')^0$		$1^4A'$	2.21	(0.92) $(19a')^1(5a'')^1(6a'')^1(20a')^0$	
$2^2A'$	2.69	(0.67) $(5a'')^1(19a')^1(6a'')^1(20a')^0$	0.04817	$2^2A'$	2.58 2.55[c]	(0.70) $(19a')^1(5a'')^1(6a'')^1(20a')^0$	0.00016
$1^4A''$	2.91	(0.91) $(5a'')^1(19a')^1(6a'')^0(20a')^1$		$2^2A''$	3.03 3.01[c]	(0.82) $(19a')^2(5a'')^0(6a'')^1(20a')^0$	0.01675
$2^2A''$	3.29	(0.79) $(5a'')^0(19a')^2(6a'')^1(20a')^0$	0.00001	$1^4A''$	3.04	(0.89) $(19a')^1(5a'')^1(6a'')^0(20a')^1$	
				$3^2A'$	3.23	(0.60) $(19a')^1(5a'')^1(6a'')^1(20a')^0$	0
				$3^2A''$	3.79	(0.60) $(19a')^0(5a'')^2(6a'')^1(20a')^0$	0.00028
		trigonal-OSSO$^+$(X^2B_2)				*lin*-OSSO$^+$($X^2\Pi_u$)	
X^2B_2	0.00	(0.92) $(1a_2)^2(12a_1)^2(4b_1)^2(7b_2)^1(5b_1)^0(13a_1)^0$		$X^2\Pi_u$	0.00	(0.85) $(2\pi_g)^4(3\pi_u)^3(3\pi_g)^0$	
1^2B_1	0.57	(0.93) $(1a_2)^2(12a_1)^2(4b_1)^1(7b_2)^2(5b_1)^0(13a_1)^0$	0	$1^4\Pi_g$	1.02	(0.92) $(2\pi_g)^4(3\pi_u)^2(3\pi_g)^1$	
1^2A_2	3.53	(0.80) $(1a_2)^1(12a_1)^2(4b_1)^2(7b_2)^2(5b_1)^0(13a_1)^0$	0.00107	$1^2\Pi_g$	1.33	(0.90) $(2\pi_g)^4(3\pi_u)^2(3\pi_g)^1$	0.00923
1^4A_2	4.33	(0.90) $(1a_2)^2(12a_1)^2(4b_1)^1(7b_2)^1(5b_1)^0(13a_1)^1$		$1^2\Phi_g$	1.75	(0.91) $(2\pi_g)^4(3\pi_u)^2(3\pi_g)^1$	0
1^4B_2	4.63	(0.89) $(1a_2)^2(12a_1)^2(4b_1)^1(7b_2)^1(5b_1)^1(13a_1)^0$		$2^2\Pi_g$	2.21	(0.90) $(2\pi_g)^4(3\pi_u)^2(3\pi_g)^1$	0.00788
				$1^4\Pi_u$	3.17	(0.89) $(2\pi_g)^4(3\pi_u)^1(3\pi_g)^2$	
				$2^2\Pi_u$	3.66	(0.87) $(2\pi_g)^4(3\pi_u)^1(3\pi_g)^2$	0
		cyc-SSOO$^+$(X^2A')					
X^2A'	0.00	(0.93) $(16a')^2(6a'')^2(7a'')^2(17a')^1(8a'')^0$					
$1^2A''$	0.38	(0.82) $(16a')^2(6a'')^2(7a'')^1(17a')^2(8a'')^0$	0				
$2^2A''$	2.36	(0.67) $(16a')^2(6a'')^1(7a'')^2(17a')^2(8a'')^0$	0				
$2^2A'$	2.65	(0.87) $(16a')^1(6a'')^2(7a'')^2(17a')^2(8a'')^0$	0.00125				
$1^4A'$	2.96	(0.90) $(16a')^2(6a'')^1(7a'')^2(17a')^1(8a'')^1$					
$3^2A'$	3.03	(0.73) $(16a')^2(6a'')^1(7a'')^2(17a')^1(8a'')^1$	0				
$1^4A''$	3.39	(0.92) $(16a')^2(6a'')^1(7a'')^1(17a')^2(8a'')^1$					
$3^2A''$	3.60	(0.55) $(16a')^2(6a'')^1(7a'')^1(17a')^2(8a'')^1$	0				

[a]We give also the dominant electronic configuration. The CI coefficient of the corresponding electronic configuration are in parentheses. The oscillator strength f is calculated between the lowest state of each isomer and the corresponding excited state. [b]For the less stable form, *trigonal*-SOOS$^+$(X^2B_2), we compute a very high density of states (>12 electronic states having energies <1.6 eV). These data are not listed here. [c]MRCI/CASSCF/aug-cc-pV(Q+d)Z vertical excitation energies.

as a radiation source. After analysis of the photoionization efficiency (PIE) spectrum of S_2O_2, they deduced an AIE of 9.93 ± 0.02 eV, which is close to the (R)CCSD(T)/aug-cc-pVTZ value (of 9.91 eV). The (R)CCSD(T)-F12/cc-pVTZ-F12 value is off by 0.1 eV, which is expected since (R)CCSD(T)-F12 is not size consistent, whereas standard (R)CCSD(T) is. Since no experimental data are available for the other structures, we recommend the (R)CCSD(T)/aug-cc-pVTZ AIEs. Moreover, Table 3 shows that we compute AIE(*cis*-OSSO) = 9.91 eV and AIE(*trans*-OSSO) = 9.87 eV. Nevertheless, both values are close to the PIE measurements by Cheng and Hung.[35] Since the formation of the S_2O_2 species in their experiments was not isomer-specific, computations suggest that both *cis*- and *trans*-OSSO are suitable candidates for the assignment of the PIE spectrum.

Table 3 shows that the AIEs of the S_2O_2 tetratomics are in the range of 9.5−12.5 eV with mostly distinct values for all species except for *cis*-OSSO and *trans*-OSSO, which have close AIEs. Indeed, we compute a difference of 0.04 eV between AIEs of the *cis*- and *trans*-forms. Nevertheless, these isomers

https://dx.doi.org/10.1021/acs.jpca.0c11407
J. Phys. Chem. A 2021, 125, 1958−1971

Table 5. Optimized Geometric Parameters at the (R)CCSD(T)/aug-cc-pV(T+d)Z and (R)CCSD(T)-F12/cc-pVTZ-F12 Level for Dicationic Isomers of [O,S,S,O][a]

method	r_1	r_2	r_3	θ_1	θ_2	θ_3	E	E_R	ADIE
				cis-$SOSO^{2+}(X^3A'')$					
RCCSD(T)	3.019	3.177	2.664	141.2	113.2	0.0	−944.75504346	0.00	24.85
RCCSD(T)-F12	3.000	3.153	2.646	141.6	112.9	0.0	−944.84064318	0.00	25.02
				trans-$SOSO^{2+}(X^3A'')$					
RCCSD(T)	3.007	3.210	2.659	141.5	105.8	180.0	−944.75241627	0.07	24.66
RCCSD(T)-F12	2.987	3.184	2.641	142.2	106.1	180.0	−944.83791358	0.07	24.83
				ring-$SOSO^{2+}(X^1A_g)$					
CCSD(T)	3.081	3.081	3.082	96.4	83.6	0.0	−944.74115368	0.38	23.92
CCSD(T)-F12	3.060	3.060	3.062	96.5	83.6	0.0	−944.82957541	0.30	24.04
				trigonal-$OSSO^{2+}(X^3A_2)$					
RCCSD(T)	2.674	4.440	2.674	109.9	109.9	0.0	−944.67094158	2.29	28.45
RCCSD(T)-F12	2.654	4.332	2.654	109.8	109.8	0.0	−944.75744763	2.26	28.78
				cyc-$SSOO^{2+}(X^3A'')$					
RCCSD(T)	2.993	3.013	4.480	60.2	100.3	−96.0	−944.60693582	4.03	27.31
RCCSD(T)-F12	2.977	2.992	4.408	60.2	100.2	−95.9	−944.68857361	4.14	27.63

[a]Bond lengths are given in Bohr, and angles are given in degrees. Relative energies (E_R) relative to the most stable species and adiabatic double ionization energies (ADIE) relative to the energy of the parent neutral isomer are given in eV.

and the others can be specifically identified in ionization experiments using, for instance, slow photo electron spectroscopy (SPES) coupled to a VUV synchrotron radiation source.[73,74] This technique is sufficiently highly resolving to distinguish between different conformers, even those presenting close AIEs as established for gas phase cytosine and peroxy radicals.[75,76] Such experimental spectra, once measured, will allow the appropriate isomers to be identified.

3.2.4. Electronic Excited States of $[S_2O_2]^+$. Table 4 presents CASSCF/aug-cc-pV(Q+d)Z vertical excitation energies of the stable cationic species. We give the energies populating the electronic states of doublet and quartet spin multiplicities up to ∼4 eV. In contrast to the neutrals, this table shows a high density of electronic states where more than 5 states are located in the 0−4 eV energy range. This high density of electronic states should favor their mutual interaction and couplings via vibronic and spin−orbit interactions. For all species except *lin*-$OSSO^+$, the first electronic excited state is located below 0.6 eV. Particularly, for the two bent structures *cis*- and *trans*-$OSSO^+$ correlating at linearity with *lin*-$OSSO^+$, the first excitation energies (0.47 and 0.37 eV, respectively) are significantly smaller than their barrier to linearity (∼1.2 eV) attesting their relative stability. In addition, the lowest quartet state is embedded into the doublet manifold. At low-energy ranges, doublet−quartet spin−orbit conversion may occur. Anyway, these processes are occurring below the first dissociation energy (1.49 eV, Figure 3), and they cannot lead to predissociation. Therefore, the low-laying doublet states are long-lived. Moreover, Table 4 shows that all the species have doublet states in the 3.1−3.9 eV range that can be accessed after absorption of photons from the corresponding ground state. Our work suggests that the near-UV absorber in the Venusian atmosphere may be due to the cations of $[S_2O_2]$ that can be obtained either after sun light ionization of $[S_2O_2]$ or after reaction between $S^+/S + SO_2/SO_2$, $O^+/O + S_2O/S_2O^+$, $O_2^+/O_2 + S_2/S_2^+$, or $SO + SO^+$. Such ions are present in the atmospheres of both Venus and Io. More in-depth investigations are needed.

3.3. Structure and Energetics of the Stable Isomers of the $[S_2O_2]^{2+}$ Dication. *3.3.1. Stable Forms of the Cationic $[S_2O_2]^{2+}$ System and Metastability.* Starting from the neutral stable isomers, we detached 2 electrons and obtained 5 stable dicationic isomers at the (R)CCSD(T)-F12/cc-pVTZ-F12 level, namely, *cis*-$SOSO^{2+}$, *trans*-$SOSO^{2+}$, *ring*-$SOSO^{2+}$ *trigonal*-$OSSO^{2+}$, and *cyc*-$SSOO^{2+}$ (in ascending order of stability). The energetic and geometric characteristics of these states are given in Table 5. All of them are located on the lowest triplet antisymmetric potential energy surface, except *ring*-$SOSO^{2+}$, which is found in the lowest symmetric singlet. Indeed, the most stable structure is the *cis*-$SOSO^{2+}$ and closely followed by the *trans*-$SOSO^{2+}$ isomer. The only singlet state found here is the *ring*-SOSO isomer (symmetry D_{2h}). For triplets, we have 1 isomer in the OSSO group (C_{2v} symmetry, *trigonal*-$OSSO^{2+}$), 2 isomers in the SOSO group (*cis*- and *trans*-$SOSO^{2+}$ in C_s symmetry), and *cyc*-$SSOO^{2+}$ (C_1 symmetry). In sum, they correspond to chains with SO central bond or to branched formaldehyde-like structure with a central S atom. We did not find chain S−S central bond structures, although they are among the most stable ones for neutral and singly charged species.

Table 5 shows that the removal of two electrons from *cis*- and *trans*-SOSO leads to an increase of the S−O−S angle close to 20° and a shortening of the terminal S−O bonds, whereas the S−O central bond is lengthened because of its weakening upon double ionization. These structural changes upon double ionization are due to the removal of the electrons from the antibonding HOMO of the SOSO species (Figure S1). For *trigonal*-OSSO, the S−S bond lengthens by almost 0.9 Bohr. For *cyc*-OSSO the S−O bond in the S−O−S plane extends by 0.9 Bohr. For the two latter forms, Coulombic repulsion between the two positive charges dominates and leads to such long S−S or S−O bonds. For *ring*-SOSO, the structure becomes flat and is of D_{2h} symmetry.

For these dications, we list in Table 6 the charge separation reaction energies forming two singly charged species. All dissociation energies are negative to release diatomic fragments and atomic plus triatomic fragments, each with one positive charge. In fact, these species are separated from their corresponding dissociation limits by large potential barriers. These dications exhibit a metastable character, which is commonly known for small doubly charged molecular compounds. For upper energies, the unimolecular decom-

https://dx.doi.org/10.1021/acs.jpca.0c11407
J. Phys. Chem. A 2021, 125, 1958−1971

Table 6. (R)CCSD(T)-F12/cc-pVTZ-F12 Reaction Energies (ΔE, in eV) of Some $S_2O_2^{2+}$ Dications Forming the Lowest Dissociation Fragments[a]

reaction	ΔE
cis-$SOSO^{2+}(X^3A'') \rightleftarrows 2\ SO^+(X^2\Pi)$	−1.59
cis-$SOSO^{2+}(X^3A'') \rightleftarrows S^+(^4S_u) + OSO^+(X^2A_1)$	−2.18
cis-$SOSO^{2+}(X^3A'') \rightleftarrows O^+(^4S_u) + SOS^+(X^2A_1)$	−3.14
trigonal-$OSSO^{2+}(X^3A_2) \rightleftarrows S_2^+(X^2\Pi_g) + O_2^+(X^2\Pi_g)$	−2.77
cyc-$SSOO^{2+}(X^3A'') \rightleftarrows S^+(^4S_u) + SOO^+(X^2A')$	−2.78

[a] ΔE is computed as the energy difference between the tetratomic dication and that of the corresponding fragments. The reaction energies of the other dicationic species can be deduced using the relative energies given in Table 5.

position of $[S_2O_2]^{2+}$ may lead to charge retaining channels (i.e., formation of a doubly charged fragment + a neutral fragment). Our data together with those available in the literature should help for their energetic localization.

3.3.2. Adiabatic Double Ionization Energies. Table 5 presents the double adiabatic ionization energies (ADIE) of neutral $[S_2O_2]$ forming the (meta)-stable dications identified here. ADIEs are deduced as the energy difference between that of the doubly charged ion and that of the corresponding neutral system after inclusion of ZPE correction. The computed values are in the range of 24−28.5 eV. No experimental data are available in the literature to compare with. Indeed, our values hence represent predictions. In contrast to AIEs, we found distinct ADIE values that can be helpful for their identification in the double ionization spectra whenever measured.

3.3.3. Pattern of the Lowest Electronic States. Table 7 shows the pattern of the electronic states of singlet and triplet multiplicities of the (meta)-stable $S_2O_2^{2+}$ dications. As for the cations, we found a high density of electronic states. Especially, this table reveals the existence of triplet states located around 3 eV that may be populated after absorption of photons from the respective triplet ground state. For *ring*-$SOSO^{2+}(^1A_g)$, we also compute an allowed singlet−singlet transition (i.e., $1^1A_u - X^1A_g$) which is at 3.64 eV. Again, such transitions fall in the near-UV Venusian absorption band. Computations suggest that dications could also be considered for the assignment of such band.

4. CONCLUSIONS

In the present contribution, we determined the stable structures of the neutral, singly, and doubly charged $[S_2O_2]$ systems and their relative stability. We also calculated their geometric parameters, fragmentation energies, and the single and double ionization energies of neutral species. Several structures are identified here for the first time, especially for the ionic species. This will help with their identification, for example, by UV spectroscopy in the laboratory or in planetary atmospheres. Computations show that in addition to *cis*-OSSO and *trans*-OSSO proposed by Frandsen et al.[11] of the absorption in the near-UV spectra of the Venusian atmosphere, other neutral S_2O_2 species and ionic $S_2O_2^+$ and $S_2O_2^{2+}$ species could contribute. Moreover, the characterization of stable singly and doubly charged S_2O_2 can also be used for their identification by mass spectrometry and in the surveys. In sum, we agree with Pérez-Hoyos et al.[14] that we are still a long way from the definitive assignment of Venus' UV absorber, since the physical chemistry of sulfur oxides in Venus atmosphere is far from being understood. Further experimental and

Table 7. Calculated Vertical Excitation Energies (ΔE in eV) for Isomers of the $[S_2O_2]^{+2}$ Dicationic System at the CASSCF/aug-cc-pV(Q+d)Z Level[a]

electronic state	ΔE	electronic configuration	f	electronic state	ΔE	electronic configuration	f
		trans-$SOSO^{2+}(X^3A'')$				*cis*-$SOSO^{2+}(X^3A'')$	
X^3A''	0.00	$(4a'')^2(18a')^2(19a')^1(5a'')^1$		X^3A''	0.00	$(4a'')^2(18a')^2(19a')^1(5a'')^1$	
$1^1A'$	1.17	$(4a'')^2(18a')^2(19a')^2(5a'')^0$		$1^1A'$	1.18	$(4a'')^2(18a')^2(19a')^2(5a'')^0$	
$1^1A''$	1.21	$(4a'')^2(18a')^2(19a')^1(5a'')^1$		$1^1A''$	1.24	$(4a'')^2(18a')^2(19a')^1(5a'')^1$	
$1^3A'$	3.37 2.97[b]	$(4a'')^2(18a')^2(19a')^0(5a'')^1(6a'')^1$	0.00020	$1^3A'$	3.64 3.27[b]	$(4a'')^2(18a')^2(19a')^0(5a'')^1(6a'')^1$ and $(4a'')^2(18a')^1(19a')^1(5a'')^2$	0.00001
$2^3A''$	3.68 3.26[b]	$(4a'')^2(18a')^2(19a')^1(5a'')^0(6a'')^1$	0.01482	$2^3A''$	4.02 3.61[b]	$(4a'')^2(18a')^2(19a')^1(5a'')^0(6a'')^1$	0.01075
		trigonal-$OSSO^{2+}(X^3A_2)$				*cyc*-$SSOO^{2+}(X^3A'')$	
X^3A_2	0.00	$(1a_2)^2(12a_1)^2(4b_1)^1(7b_2)^1$		X^3A''	0.00	$(15a')^2(16a')^2(7a'')^1(17a')^1$	
1^1A_1	1.52	$(1a_2)^2(12a_1)^2(4b_1)^2(7b_2)^0$		$1^1A''$	1.47	$(15a')^2(16a')^2(7a'')^1(17a')^1$	
1^1A_2	1.54	$(1a_2)^2(12a_1)^2(4b_1)^1(7b_2)^1$		$1^1A'$	1.48	$(15a')^2(16a')^2(7a'')^2(17a')^0$ and $(15a')^2(16a')^2(7a'')^0(17a')^2$	
1^3B_2	2.69	$(1a_2)^2(12a_1)^1(4b_1)^2(7b_2)^1$	0.00018	$1^3A'$	2.18	$(15a')^2(16a')^1(7a'')^2(17a')^1$	0.00051
1^3B_1	2.93	$(1a_2)^2(12a_1)^1(4b_1)^1(7b_2)^2$	0.00006	$2^3A''$	2.35	$(15a')^2(16a')^1(7a'')^1(17a')^2$	0.00039
		ring-$SOSO^{2+}(^1A_g)$					
X^1A_g	0.00	$(2b_{3g})^2(2b_{2g})^2(3b_{3u})^0(5b_{2u})^0$					
1^3B_{1u}	2.05	$(2b_{3g})^2(2b_{2g})^1(3b_{3u})^1(5b_{2u})^0$					
1^3A_u	2.88	$(2b_{3g})^2(2b_{2g})^1(3b_{3u})^0(5b_{2u})^1$					
1^1A_u	3.64 3.42[b]	$(2b_{3g})^2(2b_{2g})^1(3b_{3u})^0(5b_{2u})^1$	0				
1^1B_{1u}	5.05 4.61[b]	$(2b_{3g})^2(2b_{2g})^1(3b_{3u})^1(5b_{2u})^0$	0.18429				

[a] For all isomers, two excited states have been calculated in each spin symmetry. The oscillator strength f is calculated between the lowest state of each isomer and the corresponding excited state. [b] MRCI/CASSCF/aug-cc-pV(Q+d)Z vertical excitation energies.

https://dx.doi.org/10.1021/acs.jpca.0c11407
J. Phys. Chem. A 2021, 125, 1958−1971

astronomical investigations are required for which the present work serves as a guide.

■ ASSOCIATED CONTENT

Supporting Information

The Supporting Information is available free of charge at https://pubs.acs.org/doi/10.1021/acs.jpca.0c11407.

Outermost (HOMO, LUMO) molecular orbitals of S_2O_2 neutral species as computed at the HF level. Total energies (E) of the atomic, and di- and triatomic fragments calculated at the (R)CCSD(T)-F12/cc-pVTZ-F12 level. Dissociation energies (ΔE in eV) of the stable singlet and triplet isomers of $[S_2O_2]$ into two diatomics and into atom + triatom. Dissociation energies (ΔE in eV) of the stable doublet isomers of $[S_2O_2]^+$ into two diatomics and into atom + triatom. Harmonic and anharmonic frequencies of $[S_2O_2]$ species as computed at MP2/cc-pVTZ level. (PDF)

■ AUTHOR INFORMATION

Corresponding Authors

Majdi Hochlaf − *Université Gustave Eiffel, COSYS/LISIS, 77454 Champs sur Marne, France*; Email: hochlaf@univ-mlv.fr

Ridha Ben Said − *Department of Chemistry, College of Science and Arts, Qassim University, Ar Rass 58863, Saudi Arabia*; Email: ben.said.ridha@gmail.com

Gilberte Chambaud − *Université Gustave Eiffel, COSYS/LISIS, 77454 Champs sur Marne, France*; orcid.org/0000-0002-8031-2746; Email: gilberte.chambaud@u-pem.fr

Authors

Roberto Linguerri − *Université Gustave Eiffel, COSYS/LISIS, 77454 Champs sur Marne, France*; orcid.org/0000-0001-5556-0732

Mohamed Cheraki − *Université Gustave Eiffel, COSYS/LISIS, 77454 Champs sur Marne, France*

Tarek Ayari − *Université Gustave Eiffel, COSYS/LISIS, 77454 Champs sur Marne, France*

Raimund Feifel − *Department of Physics, University of Gothenburg, 412 58 Gothenburg, Sweden*

Complete contact information is available at: https://pubs.acs.org/10.1021/acs.jpca.0c11407

Notes

The authors declare no competing financial interest.

■ ACKNOWLEDGMENTS

This study was undertaken while M.H. was Waernska Guest Professor at the University of Gothenburg (Sweden). The support of this Guest Professorship is hereby gratefully acknowledged. Some of the computations were enabled by resources provided by the Swedish National Infrastructure for Computing (SNIC) at Chalmers Centre for Computational Science and Engineering (C3SE) partially funded by the Swedish Research Council through grant agreement no. 2018-05973. R.F. and M.H. acknowledge financial support from the Swedish Research Council (Sweden). This article is based upon work from COST Action CA18212 - Molecular Dynamics in the GAS phase (MD-GAS), supported by COST (European Cooperation in Science and Technology). This work was supported by a STSM Grant from COST Action CA18212.

■ REFERENCES

(1) Zhang, X.; Liang, M.-C.; Montmessin, F.; Bertaux, J.-L.; Parkinson, C.; Yung, Y. L. Photolysis of sulphuric acid as the source of sulphur oxides in the mesosphere of Venus. *Nat. Geosci.* **2010**, *3*, 834−837.

(2) Russell, C. T.; Kivelson, M. G. Detection of SO in Io's Exosphere. *Science* **2000**, *287*, 1998−1999.

(3) Holland, H. D. The oxygenation of the atmosphere and oceans. *Philos. Trans. R. Soc., B* **2006**, *361*, 903−915.

(4) Farquhar, J.; Bao, H.; Thiemens, M. Atmospheric influence of Earth's earliest sulfur cycle″. *Science* **2000**, *289*, 756−759.

(5) Kumar, M.; Francisco, J. S. Elemental sulfur aerosol-forming mechanism. *Proc. Natl. Acad. Sci. U. S. A.* **2017**, *114*, 864−869.

(6) Na, C. Y.; Esposito, L. W.; Skinner, T. E. International ultraviolet explorer observation of Venus SO_2 and SO. *J. Geophys. Res.* **1990**, *95*, 7485−7491.

(7) Barker, E. S. Detection of SO_2 in the UV spectrum of Venus. *Geophys. Res. Lett.* **1979**, *6*, 117−120.

(8) Lellouch, E.; McGrath, M. A.; Jessup, K. L. Io's atmosphere. In *Io after Galileo*; Lopes, R. M. C., Spencer, J. R., Eds.; Springer-Praxis, 2007; pp 231−264.

(9) Krasnopolsky, V. A. A photochemical model for the Venus atmosphere at 47−112 km. *Icarus* **2012**, *218*, 230−246.

(10) Marsden, C. J.; Smith, B. J. An ab initio study of many isomers of S_2O_2. A combined theoretical and experimental analysis of the harmonic force field and molecular structure of cis-planar OSSO. *Chem. Phys.* **1990**, *141*, 335−353.

(11) Frandsen, B. N.; Wennberg, P. O.; Kjaergaard, H. G. Identification of OSSO as a near-UV absorber in the Venusian atmosphere. *Geophys. Res. Lett.* **2016**, *43*, 11146−11155.

(12) Pollack, J. B.; Ragent, B.; Boese, R.; Tomasko, M.; Blamont, J.; Knollenberg, R. G.; Esposito, L. W.; Stewart, A. I.; Travis, L. Nature of the Ultraviolet Absorber in the Venus Clouds: Inferences Based on Pioneer Venus Data. *Science* **1979**, *205*, 76−79.

(13) Wu, Z.; Wan, H.; Xu, J.; Lu, B.; Lu, Y.; Eckhardt, A. K.; Schreiner, P. R.; Xie, C.; Guo, H.; Zeng, X. The near-UV absorber OSSO and its isomers. *Chem. Commun.* **2018**, *54*, 4517−4520.

(14) Pérez-Hoyos, S.; Sánchez-Lavega, A.; García-Muñoz, A.; Irwin, P. G. J.; Peralta, J.; Holsclaw, G.; McClintock, W. M.; Sanz-Requena, J. F. Venus upper clouds and the UV absorber from MESSENGER/MASCS observations. *J. Geophys. Res. Planets* **2018**, *123*, 145−162.

(15) Krasnopolsky, V. A. Disulfur dioxide and its near-UV absorption in the photochemical model of Venus atmosphere. *Icarus* **2018**, *299*, 294−299.

(16) Marcq, E.; Jessup, K. L.; Baggio, L.; Encrenaz, T.; Lee, Y. J.; Montmessin, F.; Belyaev, D.; Korablev, O.; Bertaux, J.-L. Climatology of SO_2 and UV absorber at Venus' cloud top from SPICAV-UV nadir dataset. *Icarus* **2020**, *335*, 113368.

(17) Frandsen, B. N.; Farahani, S.; Vogt, E.; Lane, J. R.; Kjaergaard, H. G. Spectroscopy of OSSO and Other Sulfur Compounds Thought to be Present in the Venus Atmosphere. *J. Phys. Chem. A* **2020**, *124*, 7047−7059.

(18) Lovas, F. J.; Tiemann, E.; Johnson, D. R. Spectroscopic studies of the SO_2 discharge system. II. Microwave spectrum of the SO dimer. *J. Chem. Phys.* **1974**, *60*, 5005.

(19) Paulse, C. D.; Poirier, R. A.; Davis, R. W. The molecular structures and harmonic force fields of SO_2, S_2O, and S_2O_2 from combined spectroscopic and SCF results. *Chem. Phys. Lett.* **1990**, *172*, 43−48.

(20) Mathies, P.; Sladky, F. O. R.; Rode, B. M. A quantum chemical investigation of CO, NF, SO, CF_2 and their combination products. *J. Mol. Struct.: THEOCHEM* **1982**, *90*, 335−340.

(21) Mayer, I.; Révész, M. Bond orders and valences in some simple sulphur compounds. *Inorg. Chim. Acta* **1983**, *77*, L205−L206.

(22) Clements, T. G.; Deyerl, H.-J.; Continetti, R. E. Dissociative Photodetachment Dynamics of $S_2O_2^-$. *J. Phys. Chem. A* **2002**, *106*, 279−284.
(23) Goodarzi, M.; Vahedpour, M.; Nazari, F. Theoretical study on the mechanism of $S_2 + O_2$ reaction. *Chem. Phys. Lett.* **2010**, *497*, 1−6.
(24) Goodarzi, M.; Vahedpour, M.; Nazari, F. Theoretical study on the atmospheric formation of cis and trans-OSSO complexes. *Chem. Phys. Lett.* **2010**, *494*, 315−322.
(25) Murakami, Y.; Onishi, S.; Kobayashi, T.; Fujii, N.; Isshiki, N.; Tsuchiya, K.; Tezaki, A.; Matsui, H. High temperature reaction of S $+SO_2 \rightarrow SO+SO$: Implication of S_2O_2 intermediate complex formation. *J. Phys. Chem. A* **2003**, *107*, 10996−11000.
(26) Ramirez-Solis, A.; Jolibois, F.; Maron, L. Born-Oppenheimer DFT molecular dynamics studies of S_2O_2: Non-harmonic effects on the lowest energy isomers. *Chem. Phys. Lett.* **2011**, *510*, 21−26.
(27) Martin-Drumel, M. A.; van Wijngaarden, J.; Zingsheim, O.; Lewen, F.; Harding, M. E.; Schlemmer, S.; Thorwirth, S. Millimeter- and submillimeter-wave spectroscopy of disulfur dioxide, OSSO. *J. Mol. Spectrosc.* **2015**, *307*, 33−39.
(28) Thorwirth, S.; Theulé, P.; Gottlieb, C. A.; Müller, H. S. P.; McCarthy, M. C.; Thaddeus, P. Rotational spectroscopy of S_2O: Vibrational satellites, ^{33}S isotopomers, and the sub-millimeter-wave spectrum. *J. Mol. Struct.* **2006**, *795*, 219−229.
(29) Delitsky, M. L.; Baines, K. H. Storms on Venus: Lightning-induced chemistry and predicted products. *Planet. Space Sci.* **2015**, *113*−*114*, 184−192.
(30) Ben Houria, A.; Ben Lakhdar, Z.; Hochlaf, M.; Kemp, F.; McNab, I. R. Theoretical investigation of the SO^{2+} dication and the photo-double ionization spectrum of SO. *J. Chem. Phys.* **2005**, *122*, 054303.
(31) Hochlaf, M.; Eland, J. H.D. A theoretical and experimental study of the SO_2^{2+} dication. *J. Chem. Phys.* **2004**, *120*, 6449−6460.
(32) Steudel, R. Schwefeloxide. In *Gmelin Handbuch der Anorganischen Chemie*, 8th ed.; Springer, Berlin, 1980; pp 1−69.
(33) Steudel, R. Sulfur-Rich Oxides S_nO and S_nO_2 ($n > 1$). *Top. Curr. Chem.* **2003**, *231*, 203−230.
(34) Ng, C. Y. In *The Structure, Energetics and Dynamics of Organic Ions*; Baer, T., Ng, C. Y., Powis, I., Eds.; Wiley: Chechister, 1996; Chapter 2, pp 35−124.
(35) Cheng, B.-M.; Hung, W.-C. Photoionization efficiency spectrum and ionization energy of S_2O_2. *J. Chem. Phys.* **1999**, *110*, 188.
(36) Field, T. A.; Slattery, A. E.; Adams, D. J.; Morrison, D. D. Experimental observation of dissociative electron attachment to S_2O and S_2O_2 with a new spectrometer for unstable molecules. *J. Phys. B: At., Mol. Opt. Phys.* **2005**, *38*, 255−264.
(37) Gu, H.; Cui, J.; Niu, D. D.; Dai, L. K.; Huang, J. P.; Wu, X. S.; Hao, Y. Q.; Wei, Y. Observation of CO_2^{2+} dication in the dayside Martian upper atmosphere. *Earth Planet. Phys.* **2020**, *4*, 1−7.
(38) Thissen, R.; Witasse, O.; Dutuit, O.; Wedlund, C. S.; Gronoff, G.; Lilensten, J. Doubly-charged ions in the planetary ionospheres: a review. *Phys. Chem. Chem. Phys.* **2011**, *13*, 18264−18287.
(39) Werner, H.-J.; Knowles, P. J.; Knizia, G.; Manby, F. R.; Schütz, M.; Celani, P.; Györffy, W.; Kats, D.; Korona, T.; Lindh, R. et al. *MOLPRO, a package of ab initio programs*, version 2015.1. http://www.molpro.net.
(40) Knowles, P. J.; Hampel, C.; Werner, H.-J. Coupled cluster theory for high spin, open shell reference wave functions. *J. Chem. Phys.* **1993**, *99*, 5219.
(41) Knowles, P. J.; Hampel, C.; Werner, H.-J. Erratum: "Coupled cluster theory for high spin, open shell reference wave functions. *J. Chem. Phys.* **2000**, *112*, 3106.
(42) Deegan, M. J. O.; Knowles, P. J. Perturbative corrections to account for triple excitations in closed and open shell coupled cluster theories. *Chem. Phys. Lett.* **1994**, *227*, 321−326.
(43) Werner, H.-J.; Adler, T. B.; Manby, F. R. General orbital invariant MP2-F12 theory. *J. Chem. Phys.* **2007**, *126*, 164102.
(44) Knizia, G.; Adler, T. B.; Werner, H.-J. Simplified CCSD(T)-F12 methods: theory and benchmarks. *J. Chem. Phys.* **2009**, *130*, 054104.
(45) Knowles, P. J.; Werner, H.-J. An efficient second-order MC SCF method for long configuration expansions. *Chem. Phys. Lett.* **1985**, *115*, 259−267.
(46) Werner, H.-J.; Knowles, P. J. A second order multiconfiguration SCF procedure with optimum convergence. *J. Chem. Phys.* **1985**, *82*, 5053−5063.
(47) Kendall, R. A.; Dunning, T. H., Jr; Harrison, R. J. Electron affinities of the first-row atoms revisited. Systematic basis sets and wave functions. *J. Chem. Phys.* **1992**, *96*, 6796.
(48) Woon, D. E.; Dunning, T. H., Jr Gaussian basis sets for use in correlated molecular calculations. III. The atoms aluminum through argon. *J. Chem. Phys.* **1993**, *98*, 1358.
(49) Dunning, T. H., Jr; Peterson, K. A.; Wilson, A. K. Gaussian basis sets for use in correlated molecular calculations. X. The atoms aluminum through argon revisited. *J. Chem. Phys.* **2001**, *114*, 9244−9253.
(50) Peterson, K. A.; Adler, T. B.; Werner, H.-J. Systematically convergent basis sets for explicitly correlated wavefunctions: the atoms H, He, B-Ne, and Al-Ar. *J. Chem. Phys.* **2008**, *128*, 084102.
(51) Hättig, C. Optimization of auxiliary basis sets for RI-MP2 and RI-CC2 calculations: Core−valence and quintuple-ζ basis sets for H to Ar and QZVPP basis sets for Li to Kr. *Phys. Chem. Chem. Phys.* **2005**, *7*, 59−66.
(52) Weigend, F. A fully direct RI-HF algorithm: Implementation, optimized auxiliary basis sets, demonstration of accuracy and efficiency. *Phys. Chem. Chem. Phys.* **2002**, *4*, 4285−4291.
(53) Klopper, W. Highly accurate coupled-cluster singlet and triplet pair energies from explicitly correlated calculations in comparison with extrapolation techniques. *Mol. Phys.* **2001**, *99*, 481−507.
(54) Werner, H.-J.; Knowles, P. J. An efficient internally contracted multiconfiguration−reference configuration interaction method. *J. Chem. Phys.* **1988**, *89*, 5803−5814.
(55) Knowles, P. J.; Werner, H.-J. An efficient method for the evaluation of coupling coefficients in configuration interaction calculations. *Chem. Phys. Lett.* **1988**, *145*, 514−522.
(56) Shamasundar, K. R.; Knizia, G.; Werner, H.-J. A new internally contracted multi-reference configuration interaction method. *J. Chem. Phys.* **2011**, *135*, 054101.
(57) Adamantides, V.; Neisius, D.; Verhaegen, G. Ab initio study of the O_4 molecule. *Chem. Phys.* **1980**, *48*, 215−220.
(58) Seidl, E. T.; Schaefer, H. F., III Is there a transition state for the unimolecular dissociation of cyclotetraoxygen (O_4)? *J. Chem. Phys.* **1992**, *96*, 1176.
(59) Peterka, D. S.; Ahmed, M.; Suits, A. G.; Wilson, K. J.; Korkin, A.; Nooijen, M.; Bartlett, R. J. Unraveling the mysteries of metastable O_4*. *J. Chem. Phys.* **1999**, *110*, 6095.
(60) Schröder, D. News about Oxygen. *Angew. Chem., Int. Ed.* **2002**, *41*, 573−574.
(61) Hernandez-Lamoneda, R.; Ramírez-Solís, A. Reactivity and electronic states of O_4 along minimum energy paths. *J. Chem. Phys.* **2000**, *113*, 4139−4145.
(62) Hernández-Lamoneda, R.; Ramírez-Solís, A. Systematic ab initio calculations on the energetics and stability of covalent O_4. *J. Chem. Phys.* **2004**, *120*, 10084.
(63) Caffarel, M.; Hernandez-Lamoneda, R.; Scemama, A.; Ramírez-Solís, A. Multireference quantum Monte Carlo study of the O_4 molecule. *Phys. Rev. Lett.* **2007**, *99*, 153001.
(64) Helm, H.; Walter, C. W. Observation of electronically excited states of tetraoxygen. *J. Chem. Phys.* **1993**, *98*, 5444.
(65) Cacace, F.; de Petris, G.; Troiani, A. Experimental Detection of Tetraoxygen. *Angew. Chem., Int. Ed.* **2001**, *40*, 4062−4065.
(66) Sormova, H.; Linguerri, R.; Rosmus, P.; Fabian, J.; Komiha, N. On the electronic states of S_4^+ and S_4^- isomer. *Collect. Czech. Chem. Commun.* **2007**, *72*, 83−89.
(67) Ndome, H.; Hochlaf, M. Ionospheric chemistry: Theoretical treatment of $ONOO^+$ and of NO_3^+. *J. Chem. Phys.* **2009**, *130*, 204301.

https://dx.doi.org/10.1021/acs.jpca.0c11407
J. Phys. Chem. A 2021, 125, 1958−1971

(68) Yeung, L. Y.; Okumura, M.; Zhang, J.; Minton, T. K.; Paci, J. T.; Karton, A.; Martin, J. M. L.; Camden, J. P.; Schatz, G. C. $O(^3P)$ + CO_2 collisions at hyperthermal energies: Dynamics of nonreactive scattering, oxygen isotope exchange, and oxygen-atom abstraction. *J. Phys. Chem. A* **2012**, *116*, 64−84.
(69) Bézard, B.; de Bergh, C. Composition of the atmosphere of Venus below the clouds. *J. Geophys. Res.* **2007**, *112*, E04S07.
(70) Alien, D.; Crisp, D.; Meadows, V. Variable oxygen airglow on Venus as a probe of atmospheric dynamics. *Nature* **1992**, *359*, 516−519.
(71) Yazidi, O.; Hochlaf, M. Generation of full dimensional potential energy surfaces for atmospherically important charge transfer tetratomic complexes: the case of the $OMgOO^+$ radical cation. *Phys. Chem. Chem. Phys.* **2013**, *15*, 10158−10166.
(72) Ndome, H.; Alcaraz, C.; Hochlaf, M. $OOCO^+$ cation I: Characterization of its isomers and lowest electronic states. *J. Chem. Phys.* **2007**, *127*, 064312.
(73) Poully, J. C.; Schermann, J. P.; Nieuwjaer, N.; Lecomte, F.; Gregoire, G.; Desfrançois, C.; Garcia, G. A.; Nahon, L.; Nandi, D.; Poisson, L.; Hochlaf, M. Photoionization of 2-pyridone and 2-hydroxypyridine. *Phys. Chem. Chem. Phys.* **2010**, *12*, 3566−3572.
(74) Briant, M.; Poisson, L.; Hochlaf, M.; de Pujo, P.; Gaveau, M.-A.; Soep, B. Ar_2 Photoelectron Spectroscopy Mediated by Auto-ionizing States. *Phys. Rev. Lett.* **2012**, *109*, 193401.
(75) Chen, Z.; Lau, K.-C.; Garcia, G. A.; Nahon, L.; Božanić, D. K.; Poisson, L.; Al-Mogren, M. M.; Schwell, M.; Francisco, J. S.; Bellili, A.; Hochlaf, M. Identifying Cytosine-Specific Isomers via High-Accuracy Single Photon Ionization. *J. Am. Chem. Soc.* **2016**, *138*, 16596−16599.
(76) Tang, X.; Lin, X.; Garcia, G. A.; Loison, J.-C.; Gouid, Z.; Abdallah, H. H.; Fittschen, C.; Hochlaf, M.; Gu, X.; Zhang, W.; Nahon, L. Identifying isomers of peroxy radicals in the gas phase: 1-$C_3H_7O_2$ vs 2-$C_3H_7O_2$. *Chem. Commun.* **2020**, *56*, 15525.

https://dx.doi.org/10.1021/acs.jpca.0c11407
J. Phys. Chem. A 2021, 125, 1958−1971